

# Preliminary Investigation of Multiplexed Pinholes with Circular Apertures and Elliptical Ports for I-123 DAT Imaging

Arda Könik, Timothy Fromme, Jan De Beenhouwer, Yulun He, Soumyanil Banerjee, Kesava Kalluri, Lars R Furenlid, and Michael A King

**Abstract—**Earlier, we proposed an inexpensive method to improve the performance of the conventional dual-head SPECT systems for I-123 dopamine transporter (DAT) imaging of Parkinson Disease. In this approach, the collimator on one head is replaced with a multi-pinhole (MPH) collimator while retaining the conventional collimator on the other head, thus enabling combined MPH/Parallelbeam (or Fanbeam) acquisition. The original MPH design consisted of 9 apertures with rectangular entrance/exit ports covering a cylindrical volume of interest (VOI) around the striatum with minimal multiplexing. Our main goal in this work is to increase the sensitivity of this system by adding more pinholes and allowing multiplexing. For a more efficient usage of the available detector coverage, we also proposed the usage of pinholes with circular apertures and elliptical ports referred to as “lofthole” herein. Circular apertures are desired because of the uniform spatial resolution, more accurate point spread function modeling and fabrication while the elliptical ports provide more flexibility in the detector coverage compared to circular ports. In this preliminary work, we present a comparison of 9, 13, 17 and 16 pinhole configurations for conic-holes (circle bases) and loftholes (circular and elliptic bases) through projections obtained from GATE Monte Carlo software.

## I. INTRODUCTION

WE have proposed a relatively inexpensive method to improve the performance of the conventional dual-camera SPECT systems for I-123 dopamine transporter (DAT) imaging by replacing one of the collimators with a specifically designed multi-pinhole (MPH) collimator [1]. The MPH focuses on the interior portion of the brain covering the striatum region at a high resolution and Fanbeam provides lower resolution, but complete sampling of the brain. The original MPH design consisted of 9 square apertures (8 oblique and 1 direct pinholes) with rectangular entrance/exit ports covering a cylindrical volume of interest (VOI) around

Manuscript received November 8, 2017. This work was supported by the National of Biomedical Imaging and Bioengineering (NIBIB) Grant No. NIH R01-EB022092. The contents are solely the responsibility of the authors and do not necessarily represent the official views of the National Institutes of Health.

Arda Könik, Timothy Fromme, Yulun He, Soumyanil Banerjee, Kesava Kalluri, and Michael A. King are with Department of Radiology, UMass Medical School, Worcester, MA, USA (e-mail: arda.konik@umassmed.edu).

Jan De Beenhouwer, University of Antwerp, imec-Vision Lab, Antwerp, Belgium.

George I. Zubal, Z-Concepts LLC, East Haven, CT, USA  
Lars R. Furenlid, <sup>4</sup>University of Arizona, Dept. of Radiology & The College of Optical Sciences, Tucson, AZ, USA

the striatum (diameter: ~12 cm and height: ~8 cm) with minimal multiplexing.

Our main goal in this work is to increase the sensitivity of the MPH component by adding more pinholes while keeping multiplexing as low as possible. For a more efficient usage of the available detector coverage (i.e., low truncation and multiplexing), we also proposed the usage of pinholes with circular apertures and elliptical ports, referred to as “lofthole” herein. Circular apertures are desired because of the uniform resolution, more accurate point spread function (PSF) modeling, and fabrication while the elliptical ports provide more flexibility in the detector coverage compared to the circular ports. A similar approach was used to obtain efficient detector coverage in [2], where lofthole had a circular aperture and a rectangular port.

Here, we present a preliminary comparison of 9, 13, 17 and 16 pinhole configurations for conic-holes (circle bases) and loftholes (circular and elliptic bases) through projections obtained from GATE Monte Carlo software [3]. For this preliminary comparison, we obtained the projection counts and multiplexing percentage.

## II. METHODS

### A. Multiple Pinhole Collimators

Using a 3D CAD software (SOLIDWORKS®) we designed MPH collimators with 9, 13, 17, and 16 pinholes for conic-hole and lofthole shapes. The aperture size was set to be 2 mm radius as determined from our previous study [4]. The 13 and 17 pinhole configurations were obtained by adding pinholes to the original 9-pinhole design and the 16-pinhole is organized in a 4x4 grid. 9,13, and 17 pinhole designs used one direct pinhole where the aperture is parallel to the collimator/detector surfaces. The rest of the pinholes are oblique where the aperture is tilted with respect to these surfaces. For the oblique pinholes, conic and lofthole entrance/exit ports were elliptic and oval, respectively. The port shapes are summarized in Fig. 1 along with the illustration of the direct pinholes (conic and lofthole).

These MPH geometries were then imported as STL format into the GATE (version 8) to obtain projections of the XCAT brain phantom [5]. The MPH designs simulated in this work are presented in Fig. 2.

PORT SHAPES	Conic	Lofthole
Direct Pinholes	Circular	Elliptic
Oblique Pinholes	Elliptic	Oval

Direct Pinhole

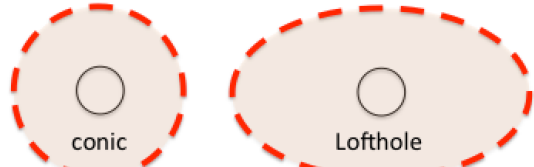


Fig. 1. Entrance/Exit port shapes for the conic and lofthole pinholes when the intersection with the collimator surface is direct (as illustrated) and oblique (not shown).



Fig. 2. MPH collimators used in the GATE simulations (front view with entrance ports). The 13 and 17 configurations were obtained by adding pinholes to the original 9 pinhole design.

### B. Projections

The default XCAT brain phantom was scaled isotropically to reflect the 99% male size and thus to show the worst possible multiplexing and truncation in the projections. The striatum (str) and background (bkg) activities were set to model I-123 DAT distribution as str:bkg=8:1. Projections of the bkg and str were obtained separately.

In Fig. 3, the projections of the XCAT brain phantom (99 percentile large male size) modeling the I-123 DAT imaging (str + bkg) are shown for the 17 and 16 pinholes.

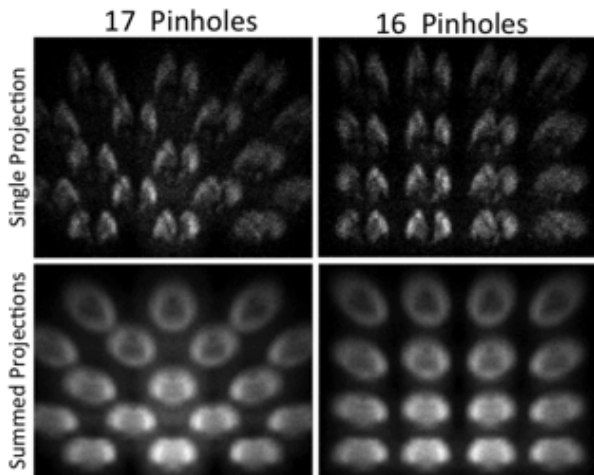


Fig. 3. Projections of the XCAT brain phantom (99% large male size) modeling the I-123 DAT imaging. These were obtained using the conic pinholes. Summed projections are from 30 equally separated views over 360°. For the 17 pinholes, there is a minor striatum/striatum overlap, while striata are well separated for the 16-pinhole configuration. Note that the projections obtained from loftholes were visually similar and are thus not presented here.

For the bkg-only projections, a set of non-multiplexing sub-projections obtained first. These background projections then summed together with different color codes as shown in Fig. 4 to illustrate the background multiplexing.

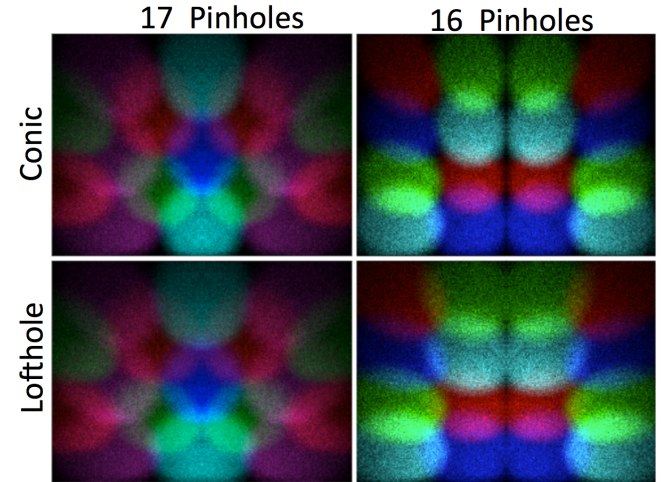


Fig. 4. Summed projections (over 360°) of the background for conic and lofthole pinholes formed from the same colored non-multiplexing sub-projections.

### C. Multiplexing

Using the non-multiplexed background projections, binary and weighted masks were obtained for each projection angle. These masks were then used to quantify bkg/bkg and bkg/str multiplexing as following:

#### Bkg/Bkg Multiplexing %

$$100 \times \sum_{\text{projection}} \text{Multiplexing Mask} \cdot \text{Bkg} / \sum_{\text{projection}} \text{Bkg}$$

#### Bkg/Striatum Multiplexing %

$$100 \times \sum_{\text{projection}} \text{Multiplexing Mask} \cdot \text{Striatum} / \sum_{\text{projection}} \text{Striatum}$$

The weighted masks account for the intensity of the background overlap and more accurately reflects the impact of multiplexing. Fig. 5 shows the weighted masks summed over 360° for all the conic and lofthole pinholes and for all the MPH configurations described here.

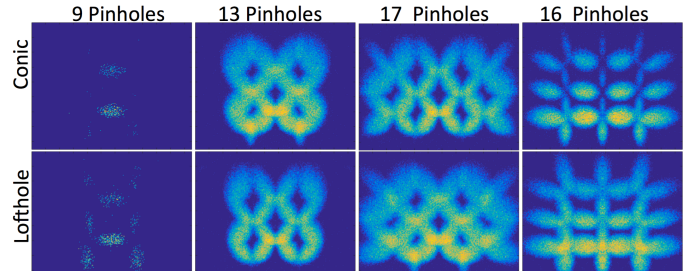


Fig. 5. Weighted masks (summed over 360° for display) showing background multiplexing. These masks are used in quantification of the background/striatum multiplexing, which represent the potential impact of multiplexing better than the use of binary masks.

### III. RESULTS

#### A. Multiplexing and Projection Counts

Table I summarizes the multiplexing% and the total counts obtained from the simulations of 4 different MPH configurations and 2 pinhole shapes. As highlighted (bold) in the table 73% sensitivity increase can be achieved in striatum counts allowing 28% background/striatum multiplexing by using the 16-conic-pinhole configuration.

TABLE I. MULTIPLEXING% AND PROJECTION COUNTS

Pinhole Type	9 Pinholes		13 Pinholes		17 Pinholes		16 Pinholes	
	Conic	Lofthole	Conic	Lofthole	Conic	Lofthole	Conic	Lofthole
Bkg/Bkg Multiplex	3%	6%	37%	44%	43%	51%	30%	41%
<b>Bkg/Str Multiplex (binary masks)</b>	<b>0%</b>	<b>0%</b>	<b>16%</b>	<b>22%</b>	<b>18%</b>	<b>24%</b>	<b>9%</b>	<b>13%</b>
<b>Bkg/Str Multiplex (weighted masks)</b>	<b>0%</b>	<b>0%</b>	<b>51%</b>	<b>70%</b>	<b>58%</b>	<b>78%</b>	<b>28%</b>	<b>41%</b>
Striatum Counts	1.5 M	1.5 M	2.3 M	2.3 M	2.7 M	2.7 M	2.6 M	2.7 M
Bkg Counts	0.9 M	1.0 M	1.4 M	1.6 M	1.9 M	2.1 M	1.3 M	1.5 M
Total Counts	2.4 M	2.5 M	3.7 M	3.9 M	4.6 M	4.8 M	3.9 M	4.2 M

### IV. DISCUSSION AND CONCLUSION

We reported the bkg/str multiplexing using binary and weighted masks. The binary masks quantify the areal overlap only. Whereas the weighted masks take into account the intensity of the overlap as well, hence more appropriately represent the potential impact of background/striatum multiplexing.

Our preliminary results appear to favor 16-conic-pinhole configuration due to lower multiplexing (28% bkg/str) and higher sensitivity gain (73%). With the usage of the lofthole pinholes we are aiming to obtain even more efficient detector coverage (minimizing truncation and multiplexing) than the usage of conic-pinholes by properly adjusting the major and minor axes of the elliptic base.

Currently, the pinholes are positioned symmetrically along the central axis and are colinear in both horizontal and vertical directions. We will alter the position and orientation of the pinholes to obtain unique views for each pinhole and improve the axial and lateral sampling by breaking the symmetry and colinearity. Ultimately, we will try to obtain the best configuration through task based performance tests on the reconstructions.

### REFERENCES

- [1] M. A. King, J. M. Mukherjee, A. Könik, I. G. Zubal, J. Dey, and R. Licho, "Design of a Multi-Pinhole Collimator for I-123 DaTscan Imaging on Dual-Headed SPECT Systems in Combination with a Fan-Beam Collimator," *Nuclear Science, IEEE Transactions on*, vol. 63, 2016.
- [2] K. Van Audenhaege, S. Vandenberghe, K. Deprez, B. Vandeghinste, and R. Van Holen, "Design and simulation of a full-ring multi-lofthole collimator for brain SPECT," *Phys Med Biol*, vol. 58, pp. 6317-36, Sep 21 2013.
- [3] S. Jan, G. Santin, D. Strul, S. Staelens, K. Assie, D. Autret, *et al.*, "GATE: a simulation toolkit for PET and SPECT," *Phys Med Biol*, vol. 49, pp. 4543-61, Oct 7 2004.
- [4] A. Könik, J. M. Mukherjee, S. Banerjee, J. De Beenhouwer, G. Zubal, and M.A. King, "Optimization of pinhole aperture size of a combined MPH/fanbeam SPECT system for I-123 DAT imaging," in *NSS/MIC*, 2016.
- [5] W. P. Segars, G. Sturgeon, S. Mendonca, J. Grimes, and B. M. Tsui, "4D XCAT phantom for multimodality imaging research," *Med Phys*, vol. 37, pp. 4902-15, Sep 2010.

### ACKNOWLEDGEMENTS

This work was supported by the National Institute of Biomedical Imaging and Bioengineering (NIBIB) Grant No. NIH R01-EB022092. The contents are solely the responsibility of the authors and do not necessarily represent the official views of the National Institutes of Health.